

## FULL PAPER

# Glucose-coated superparamagnetic nanoparticle-catalysed pyrazole synthesis in water†

Naghmeh Esfandiary | Athar Nakisa | Kobra Azizi | Jamshid Azarnia | Iman Radfar | Akbar Heydari

Tarbiat Modares University, Tehran, PO Box: 14155-4838, Iran

**Correspondence**

Akbar Heydari, Tarbiat Modares University, PO Box: 14155-4838, Tehran, Iran.  
Email: heydar\_a@modares.ac.ir

† The article is dedicated to memory of Muhammad Baqir al-Sadr.

A green, benign, heterogeneous, superparamagnetic catalyst (Glu.@Fe<sub>3</sub>O<sub>4</sub>) was synthesized and characterized using Fourier transform infrared spectroscopy, X-ray diffraction, thermogravimetric analysis, scanning electron microscopy and vibrating sample magnetometry. The prepared catalyst was used to achieve a high-efficiency, low-cost, eco-friendly and easy-to-handle protocol for synthesizing substituted pyrazole derivatives from aldehydes, malononitrile and phenylhydrazine. The catalyst was also used in chromene synthesis. Glucose coated on magnetic nanoparticles provided excellent catalytic activity. The catalyst could be recycled for up to four runs without significant loss in catalytic activity.

**KEYWORDS**

glucose immobilization, green catalyst, hydrogen bond catalysis, magnetic nanoparticles, pyrazole synthesis

## 1 | INTRODUCTION

Nowadays, scientists from all branches around the world attempt to consider their permanent home, Earth. Formulating the twelve principles of green chemistry in the 1990s was one of the first efforts in chemistry in this regard. Towards these concepts, doing reactions in mild and benign situations with the least hazards and highest synthetic efficiency is admired.<sup>[1]</sup>

Glucose is the most important monosaccharide in living organisms and it is known as the human body's key source of energy,<sup>[2]</sup> so it can be considered as a natural, biocompatible agent. As a consequence of the polyhydroxyl structure, it has been used as a green catalyst and provided excellent catalytic activity in chemical reactions<sup>[3]</sup> such as epoxidation<sup>[4]</sup> and enantioselective Michael addition.<sup>[5]</sup> Also, it has played the role of a green medium for undertaking reactions.<sup>[6]</sup> Recently, glucose-coated superparamagnetic iron oxide nanoparticles have been synthesized and used for biological applications.<sup>[7]</sup> This allows one to consider glucose-coated superparamagnetic iron oxide nanoparticles as recyclable, heterogeneous green catalysts.

Today, nanoparticles play a key role in various fields because of their unique surface-to-volume ratio that causes

interesting properties which are different from those of their bulk state.<sup>[8]</sup> In this regard, magnetic nanoparticles exhibit versatility and high-performance capabilities in various fields,<sup>[9]</sup> such as medical diagnostics and treatments,<sup>[10]</sup> chemistry,<sup>[11]</sup> wastewater treatment,<sup>[12]</sup> and so on. In terms of chemistry, their utilization as recyclable heterogeneous green nanocatalysts is of significant interest. Therefore, we decided to cover the surface of magnetic nanoparticles with glucose to make them more compatible and avoid aggregation and use the hydroxyl groups of the glucose to catalyse reactions.

Pyrazole, a five-membered heterocyclic structure, is present in many applicable components. This scaffold is found in various biomolecules with biological and pharmaceutical properties.<sup>[13]</sup> It also has been used as catalyst<sup>[14]</sup> and ligand.<sup>[15]</sup>

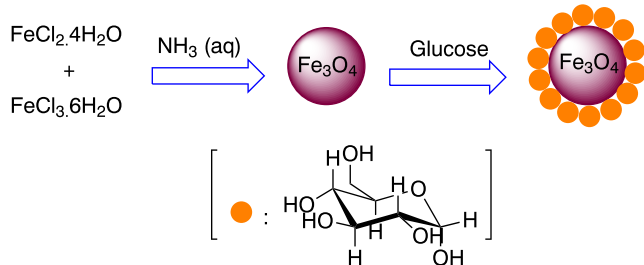
The first report of pyrazole synthesis was published in 1964, where Dickinson et al. used cyanoethylene and hydrazine to obtain aminocyanopyrazoles.<sup>[16]</sup> Later, much research has been reported of the synthesis of pyrazole with various reagents and conditions.<sup>[17]</sup> Some recent research has reported pyrazole synthesis with ionic liquid,<sup>[18]</sup> iodine<sup>[19]</sup> and metal oxide<sup>[20]</sup> as catalysts and with photocatalyst.<sup>[21]</sup> So we attempted to use our environmentally friendly catalyst to synthesize pyrazole derivatives in water at room temperature with ultrasonic irradiation.

According to the literature, the reaction of phenylhydrazine, aromatic aldehyde and malononitrile in water as solvent without catalyst at room temperature, and even under reflux conditions during 24 h, did not show any product.<sup>[20]</sup>

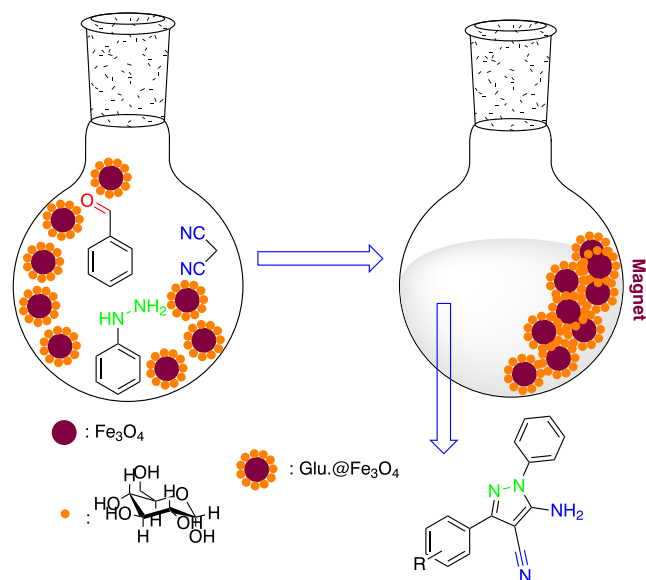
## 2 | EXPERIMENTAL

### 2.1 | Chemicals, instrumentation and analysis

All solvents and chemicals purchased were of analytical grade and used without further purification. Fourier transform infrared (FT-IR) spectra were obtained in the region



SCHEME 1 Catalyst synthetic procedure



SCHEME 2 Synthesis of pyrazoles catalysed by Glu.@Fe<sub>3</sub>O<sub>4</sub>

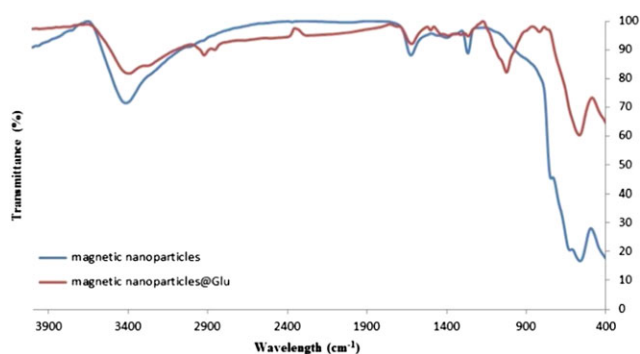


FIGURE 1 FT-IR spectra of Fe<sub>3</sub>O<sub>4</sub> and Glu.@Fe<sub>3</sub>O<sub>4</sub>

400–4000 cm<sup>-1</sup> using a Nicolet IR100 instrument with spectroscopic-grade KBr. The morphology of the catalyst was studied using scanning electron microscopy (SEM; Philips XL 30 and S-4160) with coated gold equipped with dispersive X-ray spectroscopy capability. Powder X-ray diffraction (XRD) spectra were recorded at room temperature with a Philips X-Pert 1710 diffractometer using Co K $\alpha$  radiation ( $\lambda = 1.78897 \text{ \AA}$ ) at a voltage of 40 kV and current of 40 mA to define the crystalline structure of the catalyst nanoparticles. Data were collected from 10° to 90° (2 $\theta$ ) with

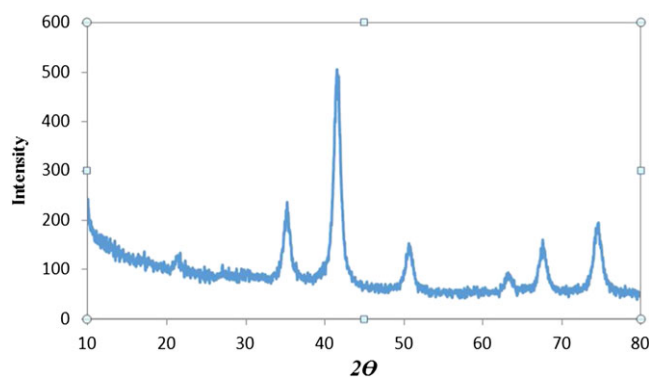


FIGURE 2 XRD pattern of Glu.@Fe<sub>3</sub>O<sub>4</sub>

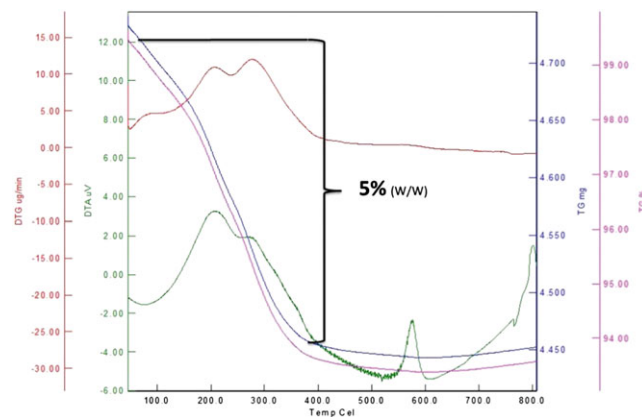


FIGURE 3 TGA of Glu.@Fe<sub>3</sub>O<sub>4</sub>

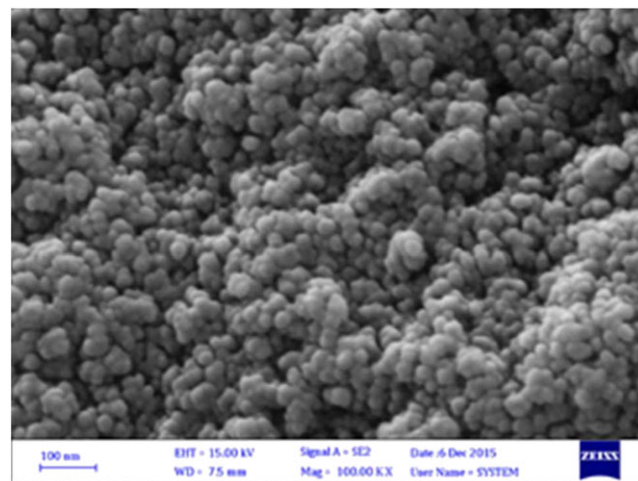


FIGURE 4 SEM image of Glu.@Fe<sub>3</sub>O<sub>4</sub>

a scan speed of  $0.02^\circ \text{ s}^{-1}$ . The magnetic properties were measured with a vibrating magnetometer/alternating gradient force magnetometer (MDCo., Iran, www.mdk-magnetic.com). Thermogravimetric analysis (TGA) was performed using a thermal analyser with a heating rate of  $20^\circ \text{ C min}^{-1}$  over the temperature range  $25\text{--}1100^\circ \text{ C}$  under flowing compressed nitrogen.

## 2.2 | Preparation of catalyst

Superparamagnetic  $\text{Fe}_3\text{O}_4$  nanoparticles were prepared according to a conventional co-precipitation method.

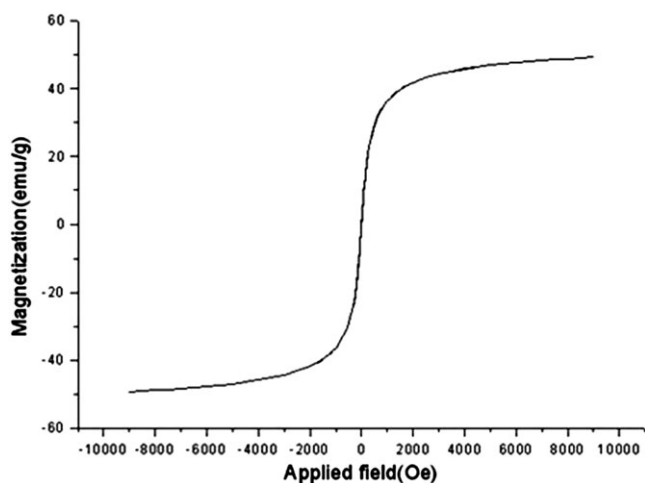
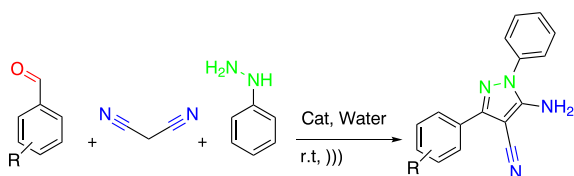


FIGURE 5 VSM curve of Glu.@ $\text{Fe}_3\text{O}_4$



SCHEME 3 Design of reaction for optimizing conditions

TABLE 1 Optimization of reaction conditions

Entry	Catalyst	Solvent	Amount of catalyst (mg)	Temp. ( $^\circ \text{C}$ )	Time (min)	Yield (%)
1	—	$\text{H}_2\text{O}$	—	r.t.	150	—
2	—	$\text{H}_2\text{O}$	—	60	20	24
3	—	$\text{H}_2\text{O}$	—	r.t./ultrasonic	20	32
4	—	$\text{H}_2\text{O}$	—	45/ ultrasonic	20	32
5	—	$\text{H}_2\text{O}$	—	60/ ultrasonic	20	32
6	Glu.@ $\text{Fe}_3\text{O}_4$	$\text{H}_2\text{O}$	20	r.t./ultrasonic	8	87
7	Glu.@ $\text{Fe}_3\text{O}_4$	$\text{H}_2\text{O}$	25	r.t./ultrasonic	8	89
8	<b>Glu.@<math>\text{Fe}_3\text{O}_4</math></b>	<b><math>\text{H}_2\text{O}</math></b>	<b>30</b>	<b>r.t./ultrasonic</b>	<b>8</b>	<b>95</b>
9	Glu.@ $\text{Fe}_3\text{O}_4$	$\text{H}_2\text{O}$	40	r.t./ultrasonic	8	95
10	Glu.@ $\text{Fe}_3\text{O}_4$	$\text{H}_2\text{O}$	50	r.t./ultrasonic	8	90
11	Glu.@ $\text{Fe}_3\text{O}_4$	MeOH	30	r.t./ultrasonic	8	87
12	Glu.@ $\text{Fe}_3\text{O}_4$	EtOH	30	r.t./ultrasonic	8	69
13	Glu.@ $\text{Fe}_3\text{O}_4$	Toluene	30	r.t./ultrasonic	15	20
14	Glu.@ $\text{Fe}_3\text{O}_4$	THF	30	r.t./ultrasonic	20	15
15	Glu.@ $\text{Fe}_3\text{O}_4$	MeCN	30	r.t./ultrasonic	15	58

$\text{FeCl}_3 \cdot 6\text{H}_2\text{O}$  (10 mmol) and  $\text{FeCl}_2 \cdot 4\text{H}_2\text{O}$  (5 mmol) salts were dissolved in 40 ml of deionized water and were stirred vigorously (800 rpm) for 2 min at room temperature. Then ammonia solution (25% w/w) was added dropwise to produce an alkaline medium (pH about 11). The obtained black suspension was stirred vigorously for 1 h at room temperature and then was refluxed for 6 h. The synthesized magnetic  $\text{Fe}_3\text{O}_4$  nanoparticles were separated from the medium by applying an external magnet and washed several times with water then ethanol. Glucose (20 mmol) was dissolved in 40 ml of deionized water and the prepared  $\text{Fe}_3\text{O}_4$  nanoparticles were added. The mixture was exposed to ultrasonic waves for 20 min. The resulting superparamagnetic nanoparticles (Glu.@ $\text{Fe}_3\text{O}_4$ ) were first separated from the alkaline medium then washed several times with deionized water then ethanol and dried at  $60^\circ \text{ C}$  overnight. The synthesis route is shown in Scheme 1.

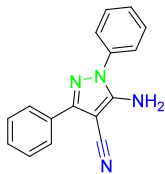
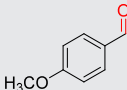
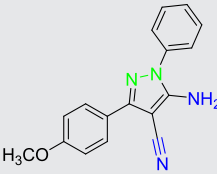
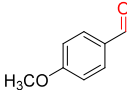
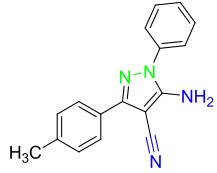
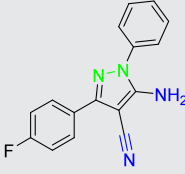
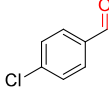
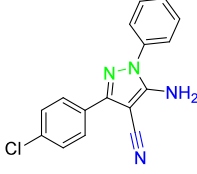
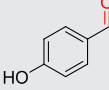
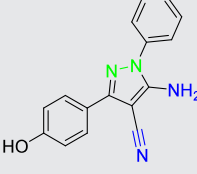
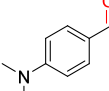
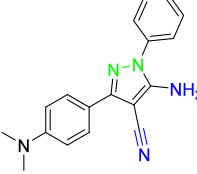
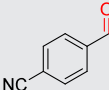
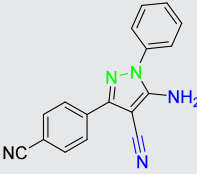
## 2.3 | General procedure for synthesis of pyrazoles

Benzaldehyde (1 mmol) and malononitrile (1 mmol) were dissolved in 1 ml of water in a round-bottom flask, and then the synthesized catalyst (30 mg) was added. To form Knoevenagel adduct, the mixture was exposed to ultrasonic waves for 2 min at room temperature. In the next step, phenylhydrazine (1 mmol) was added to afford pyrazole. After completion of the reaction, the mixture was diluted with hot ethanol, the nanocatalyst was separated from the medium with an external magnet and cold water was added to separate semi-solid products. Synthesized products were recrystallized from ethanol and then filtered under reduced pressure. The synthesis route is shown in Scheme 2.

## 2.4 | General procedure for synthesis of chromenes

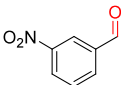
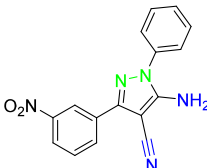
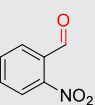
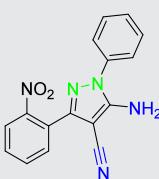
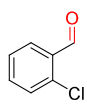
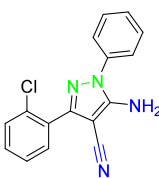
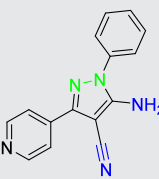
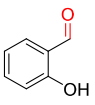
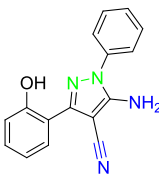
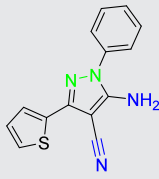
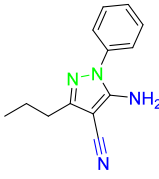
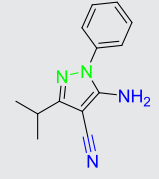
Benzaldehyde (1 mmol) and malononitrile (1 mmol) were dissolved in 1 ml of water in a round-bottom flask, and

TABLE 2 Synthesis of various pyrazole derivatives

Entry	R	Product	Time(min)	Yield (%)
1			8	95
2			6	96
3			7	90
4			5	95
5			5	95
6			7	92
7			8	89
8			6	92
9			6	99

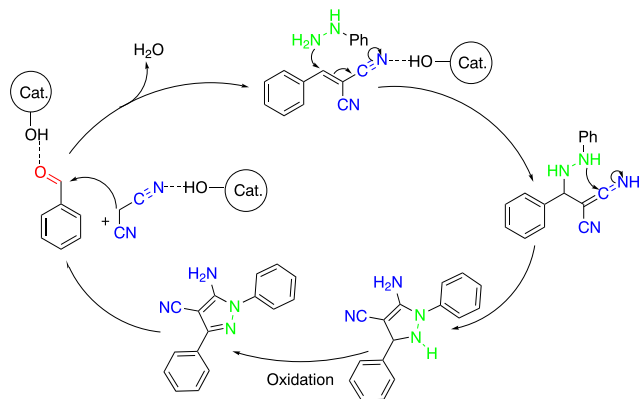
(Continues)

TABLE 2 (Continued)

Entry	R	Product	Time(min)	Yield (%)
				
10			6	98
11			7	95
12			10	94
13			8	86
14			10	93
15			—	—
16			—	—

then the synthesized catalyst (30 mg) was added. To form Knoevenagel adduct, the mixture was exposed to ultrasonic waves for 2 min at room temperature. In the next step,

$\beta$ -naphthol (1 mmol) was added to afford chromene. After completion of the reaction, the mixture was diluted with hot ethanol, the nanocatalyst was separated from the



SCHEME 4 Proposed mechanism of pyrazole synthesis

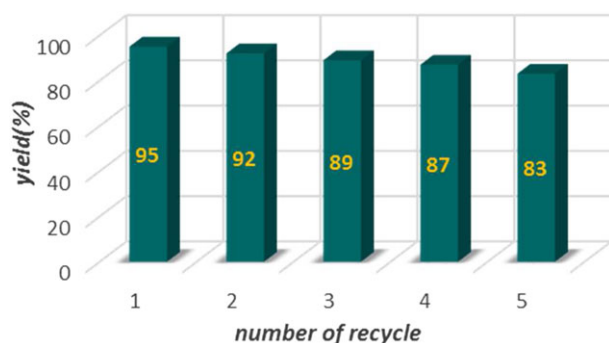


FIGURE 6 Recyclability of catalyst

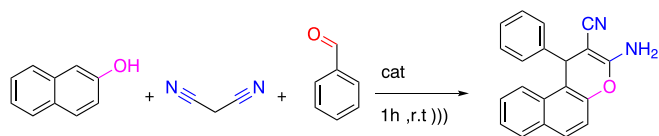
SCHEME 5 Synthesis of chromene in the presence of Glu.@Fe<sub>3</sub>O<sub>4</sub>

TABLE 3 Optimization of reaction conditions for chromene synthesis

Entry	Catalyst	Solvent	Amount of catalyst (mg)	Temp (°C)	Time (h)	Yield (%)
1	—	H <sub>2</sub> O	—	80	6	—
2	Glu.@Fe <sub>3</sub> O <sub>4</sub>	H <sub>2</sub> O	20	r.t	6	23
3	Glu.@Fe <sub>3</sub> O <sub>4</sub>	H <sub>2</sub> O	20	60	6	70
4	Glu.@Fe <sub>3</sub> O <sub>4</sub>	H <sub>2</sub> O	25	80	6	88
5	Glu.@Fe <sub>3</sub> O <sub>4</sub>	H <sub>2</sub> O	30	80	6	90
6	Glu.@Fe <sub>3</sub> O <sub>4</sub>	H <sub>2</sub> O	35	80	6	93
7	Glu.@Fe <sub>3</sub> O <sub>4</sub>	H <sub>2</sub> O	35	100	6	94
8	Glu.@Fe <sub>3</sub> O <sub>4</sub>	H <sub>2</sub> O	40	80	6	93
9	<b>Glu.@Fe<sub>3</sub>O<sub>4</sub></b>	<b>H<sub>2</sub>O</b>	<b>35</b>	<b>r.t/ultrasonic</b>	<b>1</b>	<b>93</b>
10	Glu.@Fe <sub>3</sub> O <sub>4</sub>	H <sub>2</sub> O	35	60/ultrasonic	1	94
11	Glu.@Fe <sub>3</sub> O <sub>4</sub>	H <sub>2</sub> O	35	80/ultrasonic	1	94
12	Glu.@Fe <sub>3</sub> O <sub>4</sub>	MeOH	35	80	6	88
13	Glu.@Fe <sub>3</sub> O <sub>4</sub>	EtOH	35	80	6	91
14	Glu.@Fe <sub>3</sub> O <sub>4</sub>	Toluene	35	80	6	27
15	Glu.@Fe <sub>3</sub> O <sub>4</sub>	THF	35	80	6	21
16	Glu.@Fe <sub>3</sub> O <sub>4</sub>	MeCN	35	80	6	76

medium with an external magnet and cold water was added to separate solid products. Synthesized products were recrystallized from ethanol and then filtered under reduced pressure.

### 3 | RESULTS AND DISCUSSION

To confirm the synthesis of the nanocatalyst, the structure was characterized using some spectroscopic and microscopic techniques, namely FT-IR spectroscopy, XRD, TGA, SEM and vibrating sample magnetometry (VSM).

#### 3.1 | FT-IR spectroscopy

The FT-IR spectra of magnetic nanoparticles (Fe<sub>3</sub>O<sub>4</sub>) and magnetic nanoparticles coated with glucose (Glu.@Fe<sub>3</sub>O<sub>4</sub>) are shown in Figure 1. The broad peak at 3400 cm<sup>-1</sup> is related to —OH. Peaks at 2923, 2857, 1024 and 560 cm<sup>-1</sup> are, respectively, associated with the stretching vibrations of C(sp<sup>3</sup>)—H, C(sp<sup>2</sup>)—H, C—O and Fe—O bonds.

#### 3.2 | XRD analysis

The synthesized Glu.@Fe<sub>3</sub>O<sub>4</sub> was analysed using XRD to examine the crystalline structure. The XRD pattern is shown in Figure 2. As seen, the six peaks (2θ = 35°, 43°, 51°, 63°, 67.5° and 75°) are representative of Fe<sub>3</sub>O<sub>4</sub> crystalline structure. This result proves that glucose coating does not alter the structure of the magnetic nanoparticles.

#### 3.3 | Thermogravimetric analysis

The amount of material that covers the surface of the magnetic nanoparticles was determined using TGA. As shown in Figure 3, there is only one step of weight loss, in compliance

with our consideration, which begins from under 100°C and finishes under 400°C. This decomposition appears to correspond to the loss of the organic portion (5% w/w).

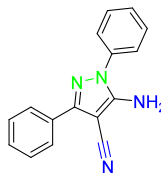
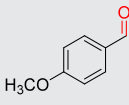
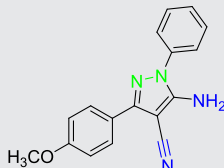
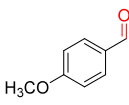
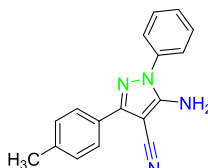
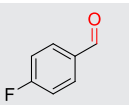
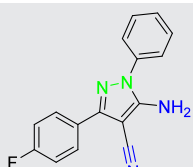
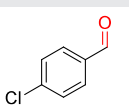
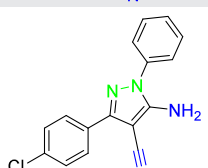
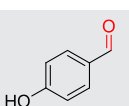
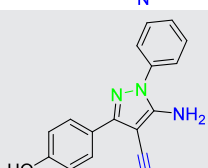
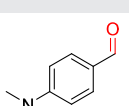
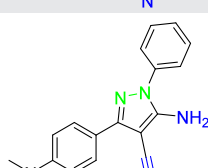
### 3.4 | SEM analysis

To investigate the surface morphology and the size of the nanoparticles, we used SEM (Figure 4). The resulting image shows uniform and minuscule nanoparticles. The approximate size of particles is determined as about 10–30 nm.

### 3.5 | VSM analysis

To investigate the magnetic properties of the nanoparticles, we used the VSM technique, applying a magnetic field in

TABLE 4 Synthesis of various chromene derivatives

Entry	Substrate	Product	Yield (%)
1			93
2			83
3			92
4			95
5			75
6			75
7			82

the range – 10 000 to +10 000 Oe at room temperature. As shown in Figure 5, the completely reversible hysteresis loop indicates the superparamagnetic property of the nanoparticles. Saturation magnetization of the nanoparticles is determined as about 52 emu g<sup>-1</sup>.

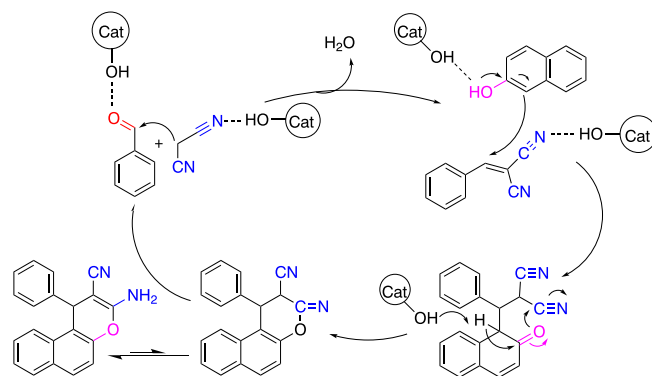
### 3.6 | Catalyst activity

The multicomponent pyrazole synthesis reaction was optimized using benzaldehyde, malononitrile and phenylhydrazine (Scheme 3) and all results are summarized in Table 1. In the first step, we attempted the reaction with no catalyst: the results are not satisfactory (entries 1–5). For the next step we tested Glu.@Fe<sub>3</sub>O<sub>4</sub> as heterogeneous catalyst and we get excellent results. So we persevered in this way to optimize other factors. We compared different media by changing solvent and observe that water leads to the best results (entries 9–15). By changing the temperature, we find the best yield is obtained when the reaction occurs at room temperature together with ultrasonication. For the last step, we find the optimized amount of catalyst is 30 mg (7 mol%) (entries 6–10).

Using this procedure, we tried to synthesize various derivatives of pyrazole using different aldehydes with malononitrile and phenylhydrazine. The achieved products are listed in Table 2.

The mechanism of this reaction, as was reported,<sup>[18]</sup> includes three steps (Scheme 4). The first step is condensation of benzaldehyde and malononitrile to obtain white crystalline Knoevenagel product. After that, phenylhydrazine is added to undergo 1,2-addition reaction, and the last step is elimination of hydrogen to cause aromaticity.

After accomplishing the reaction, the superparamagnetic nanocatalyst was separated from the medium, as usual with application of an external magnet, then washed and dried and used for another reaction run. The nanocatalyst was re-used until the results were not satisfactory. In this way, the recyclability of our synthesized nanocatalyst was examined (Figure 6). The catalyst shows excellent result for four repeat cycles, after which we witness a deterioration in its catalytic activity.



SCHEME 6 Proposed mechanism of chromene synthesis

Following the successful pyrazole synthesis, the reaction of benzaldehyde, malononitrile and  $\beta$ -naphthol was found to be facilitated, leading to the desired product in high yield (Scheme 5). The optimal reaction conditions are found to be arylaldehyde (1 mmol), malononitrile (1 mmol) and  $\beta$ -naphthol (1 mmol) at room temperature for 1 h under ultrasonic irradiation in water (Table 3, entry 9). Under these optimized conditions, various aldehydes were used as substrates for the formation of corresponding chromenes (Table 4).

The reaction mechanism consists of three steps. The first step is Knoevenagel condensation, the same as in the pyrazole synthesis reaction. The next step is Michael addition of  $\beta$ -naphthol to the Knoevenagel product. Finally the chromene product is formed by intermolecular cyclization (Scheme 6).

## 4 | CONCLUSIONS

In summary, we synthesized green benign superparamagnetic nanoparticles coated with glucose and characterized their various properties with FT-IR spectroscopy, XRD, TGA, SEM and VSM techniques. Then, we used these recyclable nanoparticles to catalyse the synthesis of pyrazole and chromene derivatives in water at room temperature under ultrasonic irradiation, as a green and environmentally friendly process.

## 5 | SPECTRAL DATA FOR SELECTED COMPOUNDS

**5-Amino-1,3-diphenyl-1H-pyrazole-4-carbonitrile.** White solid; m.p. 155–158°C. FT-IR (KBr,  $\nu_{\max}$ ,  $\text{cm}^{-1}$ ): 3440, 3311, 3028, 2261, 1595, 1444, 1258, 1134, 1065.  $^1\text{H}$  NMR (500 MHz,  $\text{CDCl}_3$ ,  $\delta$ , ppm): 7.74 (s, 1H), 7.65–7.69 (d,  $J = 8.57$  Hz, 2H), 7.37–7.40 (t,  $J = 7.71$  Hz, 2H), 7.31–7.33 (d,  $J = 6.57$  Hz, 1H), 7.28–7.30 (t,  $J = 9.00$  Hz, 2H), 7.14–7.15 (d,  $J = 7.71$  Hz, 2H), 6.88–6.91 (t,  $J = 8.28$  Hz, 1H).

**5-Amino-3-(4-hydroxyphenyl)-1-phenyl-1H-pyrazole-4-carbonitrile.** Cream solid; m.p. 177–178°C. FT-IR (KBr,  $\nu_{\max}$ ,  $\text{cm}^{-1}$ ): 3416, 3295, 3042, 2273, 1599, 1503, 1441, 1254, 1128.  $^1\text{H}$  NMR (500 MHz,  $\text{CDCl}_3$ ,  $\delta$ , ppm): 7.65 (s, 1H), 7.56–7.57 (d,  $J = 10.20$  Hz, 2H), 7.29 (b, 1H), 7.26–7.28 (t,  $J = 4.61$  Hz, 2H), 7.09–7.11 (d,  $J = 9.09$  Hz, 2H), 6.88 (b, 1H), 6.83–6.87 (t,  $J = 7.96$  Hz, 2H), 4.89 (b, 1H).

**5-Amino-3-(4-cyanophenyl)-1-phenyl-1H-pyrazole-4-carbonitrile.** Yellow solid; m.p. 157–158°C. FT-IR (KBr,  $\nu_{\max}$ ,  $\text{cm}^{-1}$ ): 3431, 3278, 3052, 2369, 1578, 1495, 1260, 1156, 1106, 1072.  $^1\text{H}$  NMR (500 MHz,  $\text{CDCl}_3$ ,  $\delta$ , ppm): 7.72–7.74 (d,  $J = 7.9$  Hz, 2H), 7.63–7.66 (t,  $J = 6.58$  Hz, 3H), 7.30–7.33 (t,  $J = 7.37$  Hz, 2H), 7.14–7.15 (d,  $J = 8.15$  Hz, 2H), 6.93–6.96 (t,  $J = 7.89$  Hz, 1H).

**5-Amino-3-(2-pyridyl)-1-phenyl-1H-pyrazole-4-carbonitrile.** Yellow-brown solid; m.p. 176–179°C. FT-IR (KBr,

$\nu_{\max}$ ,  $\text{cm}^{-1}$ ): 3149, 3126, 3024, 2954, 1743, 1571, 1492, 1278, 1142.  $^1\text{H}$  NMR (500 MHz,  $\text{CDCl}_3$ ,  $\delta$ , ppm): 8.56 (m,  $J = 7.1$  Hz, 2H), 8.04 (b, 2H), 7.51 (ddd,  $J = 6.8$  Hz, 2H), 7.22–7.33 (t,  $J = 8$  Hz, 2H), 7.10–7.16 (m,  $J = 6.5$  Hz, 2H), 6.93–7.16 (t,  $J = 7.6$  Hz, 1H).

**3-Amino-1-(thiophen-2-yl)-1H-benzo[f]chromene-2-carbonitrile (Table 4, entry 5).** FT-IR (KBr,  $\nu_{\max}$ ,  $\text{cm}^{-1}$ ): 3442, 3344, 2178, 1640, 1588.  $^1\text{H}$  NMR (500 MHz,  $\text{CDCl}_3$ ,  $\delta$ , ppm): 5.70 (s, 1H, CH), 6.87 (dd, 1H,  $J = 4.8, 3.4$  Hz), 7.01 (d, 1H,  $J = 3.3$  Hz), 7.10 (s, 2H), 7.24–7.31 (m, 2H), 7.42–7.53 (m, 2H), 7.93 (d, 2H,  $J = 8.7$  Hz), 8.03 (d, 1H,  $J = 8.2$  Hz).

## ACKNOWLEDGMENTS

We are grateful to Tarbiat Modares University for financial support of this work.

## REFERENCES

- [1] a) P. Anastas, N. Eghbali, *Chem. Soc. Rev.* **2010**, *39*, 301. b) P. T. Anastas, T. C. Williamson (Eds), *Green Chemistry: Frontiers in Benign Chemical Syntheses and Processes*, Oxford University Press, New York **1998**.
- [2] a) M. T. Gailliot, R. F. Baumeister, C. N. DeWall, J. K. Maner, E. A. Plant, D. M. Tice, L. E. Brewer, B. J. Schmeichel, *J. Pers. Soc. Psychol.* **2007**, *92*, 325. b) M. T. Gailliot, R. F. Baumeister, *Pers. Soc. Psychol. Rev.* **2007**, *11*, 303.
- [3] A. M. Faisca Phillips, *Eur. J. Org. Chem.* **2014**, *2014*, 7291.
- [4] a) T. Bakó, P. Bakó, G. Keglevich, P. Bombicz, M. Kubinyi, K. Pál, S. Bodor, A. Makó, L. Tőke, *Tetrahedron Asymm.* **2004**, *15*, 1589. b) T. K. Shing, G. Y. Leung, *Tetrahedron* **2002**, *58*, 7545.
- [5] a) L. Wang, J. Liu, T. Miao, W. Zhou, P. Li, K. Ren, X. Zhang, *Adv. Synth. Catal.* **2010**, *352*, 2571. b) Q. Gu, X.-T. Guo, X.-Y. Wu, *Tetrahedron* **2009**, *65*, 5265.
- [6] a) S. Rostamizadeh, R. Aryan, H. R. Ghaieni, *Synth. Commun.* **2011**, *41*, 1794. b) I. Yavari, E. Karimi, H. Djahaniani, *Synth. Commun.* **2007**, *37*, 2593.
- [7] D. Barbaro, L. Di Bari, V. Gandin, C. Evangelisti, G. Vitulli, E. Schiavi, C. Marzano, A. M. Ferretti, P. Salvadori, *PLoS One* **2015**, *10*, e0123159.
- [8] G. Wang, X. Su, *Analyst (Cambridge, U. K.)* **2011**, *136*, 1783.
- [9] Y. W. Jun, J. S. Choi, J. Cheon, *Chem. Commun.* **2007**, 1203.
- [10] a) V. Clavijo-Jordan, V. D. Kodibagkar, S. C. Beeman, B. D. Hann, K. M. Bennett, Wiley Interdiscip. *Rev. Nanomed. Nanobiotechnol.* **2012**, *4*, 345. b) S. C. McBain, H. H. Yiu, J. Dobson, *Int. J. Nanomedicine* **2008**, *3*, 169.
- [11] a) D. Wang, D. Astruc, *Chem. Rev.* **2014**, *114*, 6949. b) V. Polshettiwar, R. Luque, A. Fihri, H. Zhu, M. Bouhrara, J. M. Basset, *Chem. Rev.* **2011**, *111*, 3036.
- [12] a) A. Parekh, *Use of Magnetic Nanoparticles for Wastewater Treatment*, Massachusetts Institute of Technology, Cambridge, MA **2013**. b) D. K. Tiwari, J. Behari, P. Sen, *World Appl. Sci. J.* **2008**, *3*, 417. c) C. Bagheri, A. Afkhami, A. Noroozi, *Anal. Bioanal. Chem. Res.* **2016**, *3*, 1.
- [13] a) S. Manfredini, R. Bazzanini, P. Baraldi, M. Bonora, M. Marangoni, D. Simoni, A. Pani, F. Scintu, E. Pinna, L. Pisano, *Anti-Cancer Drug Des.* **1996**, *11*, 193. b) A. A. Bekhit, H. T. Fahmy, S. A. Rostom, A. M. Baraka, *Eur. J. Med. Chem.* **2003**, *38*, 27.
- [14] a) W. A. Herrmann, R. M. Kratzer, H. Ding, W. R. Thiel, H. Glas, *J. Organometal. Chem.* **1998**, *555*, 293. b) S. Chandrasekhar, T. P. Kumar, K. Haribabu, C. R. Reddy, C. R. Kumar, *Tetrahedron Asymm.* **2011**, *22*, 697.
- [15] a) T. F. S. Silva, L. M. D. R. S. Martins, M. F. C. Guedes da Silva, M. L. Kuznetsov, A. R. Fernandes, A. Silva, C. J. Pan, J. F. Lee, B. J. Hwang, A. J. L. Pombeiro, *Chem. – Asian J.* **2014**, *9*, 1132. b) W. Jin, L. Wang, Z. Yu, *Organometallics* **2012**, *31*, 5664.

- [16] C. Dickinson, J. Williams, B. McKusick, *J. Org. Chem.* **1964**, *29*, 1915.
- [17] a) C. J. Goddard, *J. Heterocycl. Chem.* **1991**, *28*, 1607. b) Y. Tominaga, Y. Matsuoka, S. Kohra, A. Hosomi, *Heterocycles* **1987**, *26*, 613.
- [18] M. Srivastava, P. Rai, J. Singh, J. Singh, *RSC Adv.* **2013**, *3*, 16994.
- [19] a) M. Srivastava, P. Rai, J. Singh, J. Singh, *New J. Chem* **2014**, *38*, 302. b) P. Rai, M. Srivastava, J. Singh, J. Singh, *RSC Adv.* **2014**, *4*, 779.
- [20] S. Maddila, S. Rana, R. Pagadala, S. Kankala, S. Maddila, S. B. Jonnalagadda, *Catal. Commun.* **2015**, *61*, 26.
- [21] Y. Ding, T. Zhang, Q. Y. Chen, C. Zhu, *Org Lett.* **2016**, *18*, 4206.

#### SUPPORTING INFORMATION

Additional Supporting Information may be found online in the supporting information tab for this article.

**How to cite this article:** Esfandiary, N., Nakisa, A., Azizi, K., Azarnia, J., Radfar, I., and Heydari, A. (2016), Glucose-coated superparamagnetic nanoparticle-catalysed pyrazole synthesis in water, *Appl Organometal Chem*, doi: 10.1002/aoc.3641